Andreev conductance in the $d+id'$-wave superconducting states of graphene

Yongjin Jiang,[1,2] Dao-Xin Yao,[2] Erica W. Carlson,[2] Han-Dong Chen,[3] and JiangPing Hu[2]
[1]*Department of Physics, ZheJiang Normal University, Jinhua, Zhejiang 321004, People's Republic of China*
[2]*Department of Physics, Purdue University, West Lafayette, Indiana 47907, USA*
[3]*Department of Physics, University of Illinois at Urbana-Champaign, Urbana, Illinois 61801, USA*
(Received 21 February 2008; revised manuscript received 22 April 2008; published 13 June 2008)

We show that effective superconducting orders generally emerge at low energy in the superconducting state of graphene with conventionally defined pairing symmetry. We study a particular interesting example, the $d_{x^2-y^2}+id'_{xy}$ spin singlet pairing state in graphene which can be generated by electronic correlation. We find that effectively the $d+id'$-wave state is a state with mixed s-wave and exotic $p+ip$-wave pairing orders at low energy. This remarkable property leads to distinctive superconducting gap functions and behavior of the Andreev conductance spectra through a normal/superconducting graphene structure.

DOI: 10.1103/PhysRevB.77.235420 PACS number(s): 74.45.+c, 74.78.Na

I. INTRODUCTION

Graphene is a single layer of hexagonally coordinated carbon atoms which has recently been isolated.[1] Due to its special lattice structure, the low-energy part of its energy spectrum is characterized by particle-hole symmetric linear dispersions around the corners of the hexagonal Brillouin zone (BZ). This band structure is responsible for many new properties of this "relativistic" condensed-matter system, such as an abnormal quantum Hall effect,[2–4] minimum conductivity,[4,5] and possibly even an experimental realization of the Klein paradox.[6]

Recently, a concept called specular Andreev reflection was proposed for a normal/superconducting (N/S) graphene interface in the context of a conventional s-wave pairing superconducting state.[7] Later, an unusual oscillation of the quantum conductance through an N/I/S junction was predicted.[8,9] The possible superconducting pairing orders in the strong correlation scenario have also been studied using the well-known resonant-valence-bond (RVB) pairing picture, which is widely adopted in layered systems with strong correlation effects. In Ref. 10, by including strong electronic correlations, the mean-field search shows that $d_{x^2-y^2}+id'_{xy}$-wave pairing symmetry is favored, similar to the superconducting state in the triangular lattice which is believed to be of $d_{x^2-y^2}+id'_{xy}$ symmetry.[11,12] In Ref. 13, an exotic $p+ip$-wave (essentially extended s-wave pairing with conventional nomenclature, see below) superconductor with spin singlet bond pairing was suggested at the mean-field level and possible phonon- or plasma-mediated mechanisms were discussed. On the other hand, experimentally, superconducting states in graphene have been realized by proximity effect[14–16] through contact with superconducting electrodes.

The peculiar physics in graphene is the unusual linear and isotropic dispersion of the low-energy excitations around the Dirac points. In this paper, we show that because of the existence of the Dirac points, conventionally defined pairing order parameters can lead to the emergence of exotic pairing states in the low-energy effective description. The $p+ip$ superconducting order of Ref. 13 is precisely such an example as an effective low-energy superconducting order, arising in that case from a more conventional extended s-wave pairing. Here, we focus on another particularly interesting superconducting state in graphene, the $d_{x^2-y^2}+id_{xy}$ spin singlet pairing superconducting state, which can be generated by electronic correlation.[10] We find that the $d+id'$-wave state is effectively a mixed s-wave and exotic $p+ip$-wave pairing states at low energy. The mixture of both s-wave and $p+ip$ wave leads to unique properties of the excitation spectrum and Andreev conductance spectra. The excitation spectrum is gapless at half-filling and is gapped away from half filling. The gap is equal to the chemical potential near half filling, and it saturates as the chemical potential is moved above the energy scale set by pairing strength. The normalized Andreev conductance in the limit of zero-bias voltage is a smooth function of the chemical potential, which starts from 2 at half filling and drops smoothly to 4/3 at large doping, unlike that in the s-wave pairing states where it almost remains at a constant value, 4/3 [see Fig. 3(c)]. This is a signature of $d_{x^2-y^2}+id'_{xy}$ pairing in graphene.

II. GENERAL PAIRING SYMMETRY AND EMERGENT PAIRING SYMMETRY AT LOW ENERGY IN GRAPHENE

A. General pairing symmetry

Although the crystal point group of graphene is D_{6h}, the pairing symmetry of the superconducting orders in a two-dimensional graphene sheet is governed by D_6, which includes four one-dimensional irreducible representations, $A_{1,2}$ and $B_{1,2}$, and two two-dimensional irreducible representations, $E_{1,2}$. Among these representations, the A_1, E_1, and E_2 representations describe s-wave, p-wave and d-wave pairing symmetries, respectively. Therefore, the spin singlet s-wave and d-wave pairings are described by the A_1 and E_2 irreducible representations. We can understand the pairing symmetry further by considering the exchange symmetry between the A and B sublattices. The D_6 group is a direct product of its two subgroups C_{3v} and Z_2, i.e., $D_6=C_{3v}\otimes Z_2$, where Z_2 describes the exchange operations between the A and B sublattices. The A_1 and E_2 representations of D_6 are symmetric under exchange of the A and B sublattices, while the E_1 representation is antisymmetric.

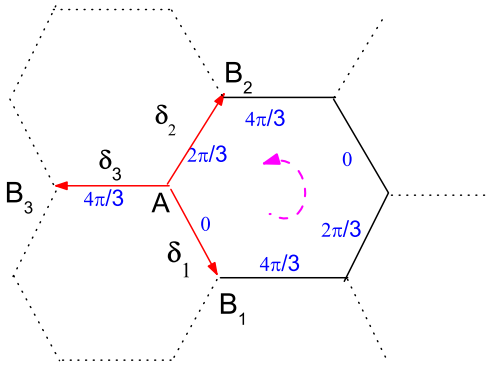

FIG. 1. (Color online) Phase (blue number) of singlet bond pairing function on the graphene lattice which preserves the translational and rotational symmetry of the honeycomb lattice and is $d+id'$ type under point group D_6. The red vectors $\vec{\delta}_a(a=1,2,3)$ denote nearest-neighbor intersublattice connections.

B. Emergent pairing symmetry at low energy

At low energy, the effective physics in graphene can be described by a relativistic dispersion near the wave vectors $\vec{K}_\pm=(0,\pm\frac{4\pi}{3\sqrt{3}})$ (hereafter subscript $\pm$ always denotes the valley index). In the superconducting state of graphene, we also have to consider the superconducting orders near these vectors at low energy, which leads to the effective superconducting orders. In particular, when the pairing is between two sublattices, the effective superconducting orders can have new pairing symmetry around the Dirac cones. To see this, consider a translationally invariant superconducting order defined on the links of the nearest-neighbor sites between the A and B sublattices. In real space, this pairing order is described by three independent values $(\Delta_{\vec{\delta}_1},\Delta_{\vec{\delta}_2},\Delta_{\vec{\delta}_3})$, as shown in Fig. 1. In momentum space, the superconducting order is given by

$$\Delta(\vec{k})=\sum_a \Delta_{\vec{\delta}_a} e^{i\vec{k}\cdot\vec{\delta}_a}. \tag{1}$$

At low energy, near the Dirac cones, the effective superconducting order is given by $\Delta_\pm(\vec{q})=\Delta(\vec{K}_\pm+\vec{q})$. Given a small $\vec{q}$, we have

$$\Delta_\pm(\vec{q})=\Delta(\vec{K}_\pm)+i\vec{q}\cdot\left(\sum_a \vec{\delta}_a\Delta_{\vec{\delta}_a}e^{\pm i\vec{K}_\pm\cdot\vec{\delta}_a}\right). \tag{2}$$

Let us consider two specific cases. The first case is extended s-wave pairing. In this case, $\Delta_{\vec{\delta}_a}=\Delta$, $a=1,2,3$. The first term on the right side of Eq. (2) vanishes and it is easy to show that $\Delta^s_\pm(\vec{q})=-\frac{3}{2}\Delta(\pm q_y+iq_x)$, which becomes a p-wave-like pairing order. Therefore, the extended s-wave pairing order in graphene at low energy is described by two $p+ip$ pairing orders that are connected with each other by time-reversal symmetry. This case has been studied in Ref. 13. The second case is $d_{x^2-y^2}+id'_{xy}$ wave pairing on which this paper is focused. In this case, $\Delta_{\vec{\delta}_i}=\Delta e^{2ia\pi/3}$, $a=1,2,3$. The effective superconducting orders for small $\vec{q}$ in Eq. (2) become

$$\Delta^d_+(\vec{q})=3\Delta e^{i4\pi/3},$$

$$\Delta^d_-(\vec{q})=\frac{3}{2}e^{i\pi/3}\Delta(iq_x+q_y). \tag{3}$$

The first equation, $\Delta^d_+(\vec{q})$, corresponds to s-wave pairing, and the second, $\Delta^d_-(\vec{q})$, to $p+ip$-wave pairing. Therefore, *at low energy*, the $d_{x^2-y^2}+id'_{xy}$ wave pairing state in graphene is a superconducting state with mixed s and $p+ip$ pairing orders.

III. LATTICE MODEL AND THE QUASIPARTICLE SPECTRUM IN MEAN FIELD DESCRIPTION

The graphene system is composed of two sublattices which are labeled as A and B, as shown in Fig. 1. If the superconducting pairing is between two sublattices, the pairing Hamiltonian can be written at the mean-field level as follows:[10,17]

$$H=-t\sum_{i,a,\sigma}[A^\dagger_{i\sigma}B_{i+\vec{\delta}_a\sigma}+\text{H.c.}]+\sum_{i,a}[\Delta_{\vec{\delta}_a}(A^\dagger_{i\uparrow}B^\dagger_{i+\vec{\delta}_a\downarrow}-A^\dagger_{i\downarrow}B^\dagger_{i+\vec{\delta}_a\uparrow})+\text{H.c.}]-\mu\sum_{i,\sigma}(A^\dagger_{i\sigma}A_{i\sigma}+B^\dagger_{i+\vec{\delta}_1\sigma}B_{i+\vec{\delta}_1\sigma}), \tag{4}$$

where the index i sums over sites on the A sublattice. $A^\dagger_{i\sigma}$ and $B^\dagger_{j\sigma}$ are creation operators for two sublattices and $\sigma=\uparrow,\downarrow$ are spin indices. The first term describes free band where $t\sim 2.8$ eV is the nearest-neighbor hopping constant. In the pairing term, $\Delta_{\vec{\delta}_a}$ is the spin singlet bond pairing order parameter, which has $d+id'$ symmetry under the point group D_6, i.e., $\Delta_{\vec{\delta}_a}=\Delta e^{2ia\pi/3}$, where Δ is the pairing strength. The phase of the order-parameter winds by 4π around each hexagonal plaquette (shown in Fig. 1). This ansatz preserves the rotational and translational symmetries of the original lattice but breaks time-reversal symmetry (TRS) manifestly. The chemical potential μ can be tuned by the gate voltage.

In momentum space, we can rewrite the Hamiltonian in the form $H=\Sigma_{\vec{k}}\Psi^\dagger_{\vec{k}}\tilde{H}_{\vec{k}}\Psi_{\vec{k}}+\text{const}$, where we defined the Nambu spinor $\Psi_{\vec{k}}=(A_{\vec{k}\uparrow},B_{\vec{k}\uparrow},A^\dagger_{-\vec{k}\downarrow},B^\dagger_{-\vec{k}\downarrow})$ and the 4×4 matrix $\tilde{H}_{\vec{k}}$ is

$$\tilde{H}_{\vec{k}}=\begin{pmatrix}-\mu & f(\vec{k}) & 0 & \Delta(\vec{k})\\ f(\vec{k})^* & -\mu & \Delta(-\vec{k}) & 0\\ 0 & \Delta(-\vec{k})^* & \mu & -f(-\vec{k})^*\\ \Delta(\vec{k})^* & 0 & -f(-\vec{k}) & \mu\end{pmatrix}, \tag{5}$$

where the function $f(\vec{k})$ is defined by $f(\vec{k})=-t\Sigma_a e^{i\vec{k}\cdot\vec{\delta}_a}$ and $\Delta(\vec{k})$ is defined by Eq. (1).

The elementary excitation spectrum of mean Hamiltonian [Eq. (5)] can be obtained through Bogoliubov diagonalization as

$$E(\vec{k}) = \pm \sqrt{\mu^2 + \epsilon_k^2 + \frac{1}{2}(g_+^2 + g_-^2) \pm \frac{1}{2}\sqrt{(g_+^2 - g_-^2)^2 + 4\epsilon_k^2(g_+^2 + g_-^2) + 16\epsilon_k^2\mu^2 - 8\,\mathrm{Re}(f(k)^2 g(-k) g(k)^*)}}, \quad (6)$$

where we defined $g_\pm = |\Delta(\pm k)|$ and the free band energy $\epsilon_k = t\sqrt{3+2\cos(\sqrt{3}k_y)+4\cos(\frac{1}{2}k_x)\cos(\frac{\sqrt{3}}{2}k_y)}$. It is well known that the low-energy part of ϵ_k has a form of Dirac cones centered around the hexagonal corners of the BZ. Only two types of these cones are inequivalent and the low-energy physics is usually described by the degenerate double-Dirac-cone structure, which is also called valley isospins in literature.

In Eq. (5), the superconductivity pairing order parameter mixes A sublattice component of spin-up states in one valley to the B sublattice component of spin-down states in the other valley. This is reflected in the off-diagonal structure of the pairing elements in Eq. (5), which will be discussed later.

In our scheme, six corners of BZ are coordinated as $(0, \pm 4\pi/3\sqrt{3})$ and $(\pm 2\pi/3, \pm 2\pi/3\sqrt{3})$. It can be easily check that ϵ_k vanishes on all these points. Furthermore, g_+ is zero in three of these corners (one valley), and g_- vanish at other three (another valley) corners. It can be seen from Eq. (6) that the properties of ϵ_k and $g_\pm$ functions ensure gapless excitation at half filling ($\mu=0$) for any pairing strength.

From Eq. (6), we can obtain the minimum of the excitation energy, which we will call the energy gap E_{gap} throughout this paper. It can be shown rigorously that for $\mu \ll \Delta$ and $E_{\mathrm{gap}} = \mu$. In Fig. 2 we plot the gap as a function of chemical potential. E_{gap} is linear in the $\mu \ll \Delta$ (low doping) region and saturates to a constant $E_{\mathrm{gap}}^{\mathrm{sat}}$ for $\mu \gg \Delta$. This unique dependence of the energy gap on the chemical potential in the $d+id'$ superconducting state stems from the mixture of the s wave and the $p+ip$ wave components. The $p+ip$-wave component dominates at low doping; thus, the gap depends linearly on the chemical potential, similar to the gap behavior reported in Ref. 13 (where the gap is proportional to $\mu\Delta$, which is quantitatively different from our case). On the other hand, the s-wave component dominates in the high doping region, the gap saturates above the s-wave superconducting order-parameter strength. The evolution of gap function clearly reflects the mixed pairing structure, which is a fascinating feature of the concept of effective pairing order here.

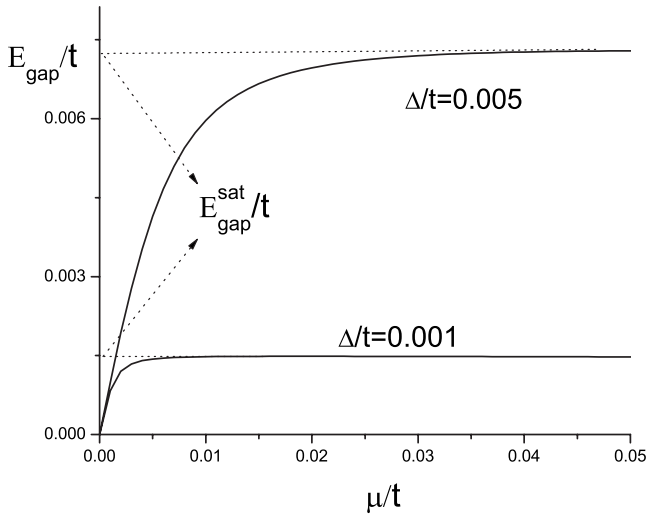

FIG. 2. The energy gap E_{gap} as a function of chemical potential for pairing strength $\Delta=0.001$t and $\Delta=0.005$t, i.e., ~3 mev and ~15 mev separately. Notably, E_{gap} is linear at low doping region and saturates to a constant $E_{\mathrm{gap}}^{\mathrm{sat}}$ when $\mu \gg \Delta$.

IV. LINEARIZED FORM

At low energy, we can linearize the mean-field Hamiltonian [Eq. (5)] near the two inequivalent BZ corners $\vec{K}_\pm$. Near $K_\pm$, $f(\vec{K}_\pm + \vec{k})$ can be expanded as

$$f_\pm(\vec{k}) = f(\vec{K}_\pm + \vec{k}) = v(ik_x \pm k_y), \quad (7)$$

where we introduced a valley dependent function $f_\pm$ and the velocity of the Dirac particles is denoted to be $v = \frac{3t}{2}$. Note hereafter k_x, k_y always refer to the relative vectors measured from $K_\pm$. By substituting Eqs. (3) and (7) into Eq. (5), we obtain

$$\tilde{H}_\pm(\vec{k}) = \begin{pmatrix} v(\pm k_y\sigma_x - k_x\sigma_y) - \mu & \tilde{\Delta}_\pm(\vec{k}) \\ \tilde{\Delta}_\pm^\dagger(\vec{k}) & \mu - v(\pm k_y\sigma_x - k_x\sigma_y) \end{pmatrix}, \quad (8)$$

where $\sigma_{x,y}$ refer to the Pauli matrices. The linearized pairing matrices $\tilde{\Delta}_\pm(\vec{k})$ for the "$\pm$" valleys take the form

$$\tilde{\Delta}_+(\vec{k}) = \Delta \begin{pmatrix} 0 & 3e^{i4\pi/3} \\ \frac{3}{2}(-ik_x - k_y)e^{i\pi/3} & 0 \end{pmatrix}, \quad (9)$$

and $\tilde{\Delta}_-(\vec{k}) = \tilde{\Delta}_+(-\vec{k})^T$. In Eq. (8), $\tilde{H}_\pm(\vec{k})$ refer to the pairing Hamiltonian between one state with wave vector $\vec{k}$ belonging to $\pm$ valley and another state with wave vector $\vec{k}$ belonging to $\mp$ valley. It can be easily checked that the valley-dependent Hamiltonian $\tilde{H}_+(\vec{k})$ and $\tilde{H}_-(-\vec{k})$ transform into each other under lattice inversion, $A_{\vec{k}} \rightleftharpoons B_{-\vec{k}}$. Here we note that the $d+id'$ pairing ansatz break TRS but preserves inversion symmetry so that the valley degeneracy is unbroken.

The diagonal part of Eq. (8) is different from the familiar form used in the Dirac–Bogoliubov–de Gennes (DBDG) equation[7] only by one step, i.e., a unitary transformation $e^{i\pi/4\sigma_z}$. One notable difference between Eq. (8) and the correspondent form in those DBDG theories is that the pairing matrix $\tilde{\Delta}$ is off-diagonal in our case, describing intersublattice pairing, while in the previous studies the assumed pairing matrix is diagonal and describe intrasublattice pairing.

In Eq. (9), the mixed pairing order of s wave and $p+ip$ wave is manifestly shown. Such mixed nature of pairing or-

der is absent in both conventional s-wave DBDG theories[7] and RVB-like extended s-wave theory.[13] In Sec V, we will show that due to this mixed order, the Andreev conductance spectra will show some qualitative deviation to those cases with pure pairing order.

V. ANDREEV CONDUCTANCE THROUGH S/N JUNCTION

In the following, we show that the mixture of the s wave and $p+ip$ wave in the $d+id'$ superconducting state of graphene results in a distinctive signature in the Andreev conductance spectra. Consider a S/N graphene junction with the $x<0$ region being the graphene $d+id'$ superconductor and the $x>0$ region being the normal state of graphene. We assume that the electrostatic potential on the S side is lower than that on the N side by a value $U_0>0$, which can be fixed through the gate voltage or by doping. A large U_0 implies a heavily doped superconductor. Due to the spin and valley degeneracy, we can restrict the incident state from N side to be spin up and from valley + and multiply the conductance by 4 at the end.

Under certain voltage bias V, we expect the incidence of a particle excitation with energy $\varepsilon=eV$ from the $x>0$ side onto the junction at $x=0$. The general form of the incident wave function is $\Psi_i^e=\Phi^e(-k_x,k_y)e^{i(-k_x x+k_y y)}$, where $k_x(k_y)$ is the longitudinal (transverse) component of the wave vector. In the scattering process, we assume energy and the transverse component of the wave vector is conserved. The reflected states can be either an electron state $\Psi_r^e=\Phi^e(k_x,k_y)e^{i(k_x x+k_y y)}$ or a hole state $\Psi_r^h=\Phi^h(k_x',k_y)e^{i(k_x' x+k_y y)}$, where k_x' is determined by $vk'=|\varepsilon-E_F|$; it is negative for $\varepsilon<E_F$ (retroreflection) and positive for $\varepsilon>E_F$ (specular reflection).[7] It can also be imaginary if $vk_y>|\varepsilon-E_F|$ and the corresponding hole state is an evanescent state near the boundary. Φ^e and Φ^h are four-component spinor eigenstates of Eq. (8) on N side (for which $\Delta=0$) corresponding to electron and hole excitations, respectively.

On the S side, we diagonalize Eq. (8) and obtain the Bogoliubov quasiparticle states. The general form of the quasiparticle states on the S side is denoted by $\Phi^s(k_x^s,k_y)e^{i(k_x^s x+k_y y)}$, where k_x^s is the longitudinal component of the wave vector on the S side. The four-component spinor $\Phi^s(k_x^s,k_y)$ is called electronlike (holelike) if the summation of the square of absolute values of the first two components is larger (lesser) than that of the last two components. For each ε and k_y, we can obtain four quasi-particle states. Two quasiparticle states are picked out among four. The chosen states satisfy one of the following three conditions: (1) k_x^s is real and positive and $\Phi^s(k_x^s,k_y)$ is holelike, (2) k_x^s is real and negative and $\Phi^s(k_x^s,k_y)$ is electronlike, and (3) k_x^s is complex and the imaginary part is negative. The last case corresponds to evanescent states near the interface. By matching the wave functions of both sides at the interface $x=0$, we can obtain the reflection coefficients r and r_A for states Ψ_r^e and Ψ_r^h, respectively. The quantum conductance through the S/N junction can be calculated using the Blonder-Tinkham-Klapwijk formula,[18]

$$G = G_0 \int_0^{\pi/2} (1 - |r(eV,\alpha)|^2 + n_h |r_A(eV,\alpha)|^2) \cos\alpha d\alpha, \tag{10}$$

where $\alpha=tg^{-1}(\frac{k_y}{k_x})$ is the incident angle and $G_0=\frac{4e^2}{h}N(eV)$ is the ballistic conductance of the graphene sheet with density of states $N(eV)=\frac{(E_F+eV)W}{v\pi}$ (where W is the width of the graphene sheet). n_h equals 1 if the hole state on the N side is propagating, and it is 0 if the state is evanescent.

For ease of comparing our results with the s-wave results in Ref. 7, we depict the normalized quantum conductance G/G_0 (as a function of bias voltage) of the S/N junction with the S side being heavily doped superconducting graphene for two cases, i.e., for $E_F>E_{\text{gap}}^{\text{sat}}$ and $E_F<E_{\text{gap}}^{\text{sat}}$ in Figs. 3(a) and 3(b), respectively, where $E_{\text{gap}}^{\text{sat}}$ is the saturated gap for $\mu\gg\Delta$ shown in Fig. 2.

For $E_F>E_{\text{gap}}^{\text{sat}}$, G/G_0 monotonically decreases in the region $eV<\Delta$ and saturates to a constant value quickly as $eV>\Delta$. The saturation value slightly decreases with E_f. For $E_f<E_{\text{gap}}^{\text{sat}}$, the line shape is similar to the s-wave case, except that the unbiased conductance is nearly 2 instead of $\frac{4}{3}$. It is noteworthy that G/G_0 is always zero at the point $E_f=eV$ in Fig. 3(b) since there is no Andreev hole reflected back at this point for any angle of incidence.

The most remarkable difference between the G/G_0-eV curves for the conventional s-wave case[7] and the $d+id'$ wave case in this paper is the value of the unbiased conductance, i.e., $\frac{4}{3}$ for s wave and nearly 2 for our case. In Ref. 7, the lines are calculated in the large U_0 limit. To make things more clear, we calculated the unbiased G/G_0 as a function of U_0 with several different choices of E_f and Δ values. In Fig. 3(c), we plot a typical comparison for three kinds of pairing order parameters. The results for the conventional s-wave[7] and RVB-like extended s-wave[13] cases show little difference. For both cases the unbiased G/G_0 quickly converges to the value of 4/3. However, for the $d+id'$ wave case considered here, G/G_0 decreases slowly from 2 and converges to 4/3 after $U_0>10t$, which is far beyond the single band edge.

The most fundamental difference between the $d+id'$ pairing ansatz and other ansatz is that it breaks time-reversal symmetry and has an emergent mixed s-wave and p-wave pairing at low energy. In combination with gap function behavior discussed above, we conclude that the mixed pairing order plays an important role in determination of the superconducting properties of graphene. It would be interesting to mention that in a recent conductance measurement on a S/N/S structure, which is a realization of Andreev billiards, the Andreev conductance is always peaked at zero voltage bias.[15] This result is qualitatively consistent with our calculation and may shed new light on the superconducting pairing symmetry of the graphene.

VI. REALIZATION OF $d+id'$-WAVE SUPERCONDUCTING STATE IN GRAPHENE

It has been shown that the $d+id'$-wave superconducting state in graphene is a natural mean-field solution in the presence of strong electron correlation.[10] Actually, the honey-

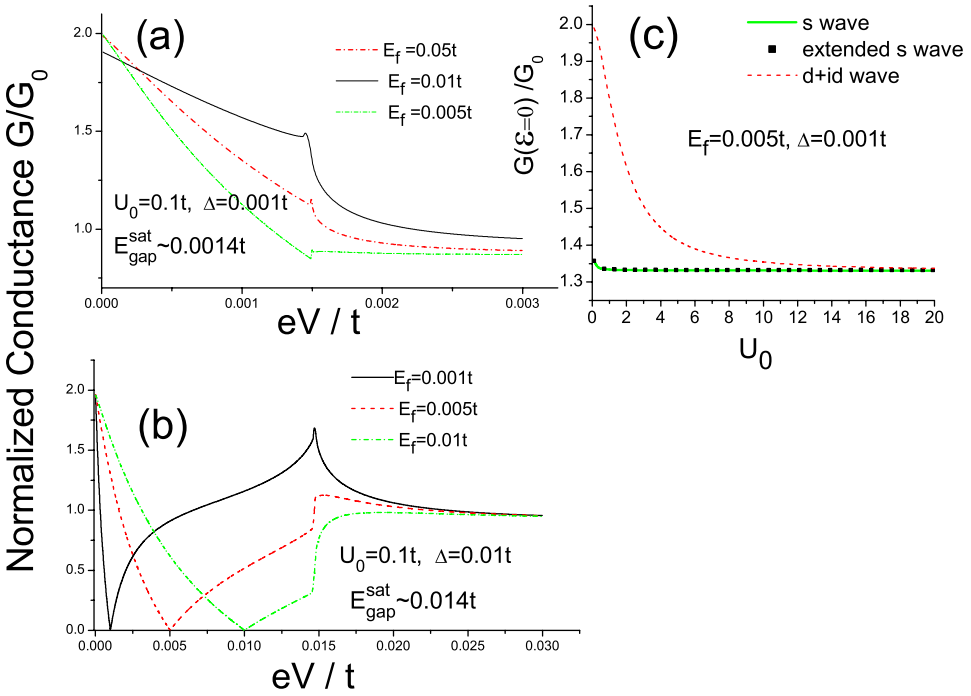

FIG. 3. (Color online) The normalized quantum conductance of a S/N graphene junction is shown in (a) with $E_f > E_{gap}^{sat}$ and (b) with $E_f < E_{gap}^{sat}$ for heavily doped superconductor ($U=0.1t$, ~ 280 meV). Also shown in (c) is the normalized conductance for zero-bias voltage for three kinds of pairing order parameters, i.e., conventional s wave, extended s wave (bond pairing), and $d+id'$ wave (bond pairing).

comb lattice is closely related to triangular lattice (with same lattice rotational symmetry), in which the superconducting state is believed to be of $d \pm id'$.[11,12] Although the electron correlation in graphene is probably not strong enough to produce a $d+id'$ superconducting by itself, it is possible to realize the $d+id'$ superconducting state by including the proximity effect through a connection to another superconductor. So far all experimental reports on superconducting properties are obtained in graphene samples contacted with normal superconductor electrodes.[14,15] The proximity effect must play an essential role on realizing superconductivity on graphene. However, the actual pairing (nonuniform in realistic cases) form may also be influenced by electron correlation. Due to the presence of weak electron correlation effect, it is possible that even a s-wave superconductor may induce $d+id'$ order, as the conductance measurement[15] that we mentioned earlier indicates. Furthermore, we can envisage the possible realization of $d+id'$ superconducting state by putting a d-wave cuprate superconductor on top of a graphene sheet (a systematic understanding of Andreev conductance in a closed related semiconductor/superconductor hybrid structure can be found in Ref. 19 and references therein). In the long-wavelength description, the effect of lattice mismatch is irrelevant and $d+id'$-wave superconducting state may also be induced. The immediate consequence of the presence of the $d+id'$ order is the spontaneous supercurrent along the interface. A self-consistent study of such proximity effect will be presented elsewhere.

VII. SUMMARY

In summary, we have shown that a combination of s-wave and $p+ip$-wave pairing order parameters emerges at low energy in the spin singlet nearest-neighbor resonant-valence-bond pairing superconducting state of $d_{x^2-y^2}+id'_{xy}$ symmetry in graphene. This mixture of s-wave and $p+ip$-wave results in (a) distinctive superconducting gap which changes linearly with chemical potential (dominated by $p+ip$-wave component, see Ref. 13) near Dirac energy and saturates at constant energy at larger chemical potential (dominated by conventional s-wave component) and (b) behavior of the Andreev conductance spectra, which differs qualitatively from the Andreev conductance spectra obtained with a purely s-wave pairing as well as $p+ip$-wave pairing superconducting state.

ACKNOWLEDGMENTS

Y.J.J. and J.P.H. are supported by the National Science Foundation (Grant No. PHY-0603759) and Natural Science Foundation of Zhejiang province (Grant No. Y605167) of China. D.X.Y. is supported by Purdue University and Research Corporation. EWC is a Cottrell Scholar of Research Corporation. H.D.C. is supported by the DOE Award No. DEFG02-91ER45439, through the Frederick Seitz Materials Research Laboratory at UIUC.

[1] K. S. Novoselov, A. K. Geim, S. V. Morozov, D. Jiang, Y. Zhang, S. V. Dubonos, I. V. Grigorieva, and A. A. Firsov, Science **306**, 666 (2004).
[2] K. S. Novoselov, A. K. Geim, S. V. Morozov, D. Jiang, M. I. Katsnelson, I. V. Grigorieva, S. V. Dubonos, and A. A. Firsov, Nature (London) **438**, 197 (2005); Yuanbo Zhang, Yan-Wen Tan, Horst L. Stormer, and Philip Kim, *ibid.* **438**, 201 (2005).
[3] V. P. Gusynin and S. G. Sharapov, Phys. Rev. Lett. **95**, 146801 (2005).
[4] N. M. R. Peres, F. Guinea, and A. H. Castro Neto, Phys. Rev. B **73**, 125411 (2006).
[5] M. I. Katsnelson, Eur. Phys. J. B **51**, 157 (2006); J. Tworzydlo, B. Trauzettel, M. Titov, A. Rycerz, and C. W. J. Beenakker, Phys. Rev. Lett. **96**, 246802 (2006); K. Nomura and A. H. MacDonald, *ibid.* **98**, 076602 (2007); I. L. Aleiner and K. B. Efetov, *ibid.* **97**, 236801 (2006); A. Altland, *ibid.* **97**, 236802 (2006).
[6] M. I. Katsnelson, K. S. Novoselov, and A. K. Geim, Nat. Phys. **2**, 620 (2006).
[7] C. W. J. Beenakker, Phys. Rev. Lett. **97**, 067007 (2006); C. W. J. Beenakker, arXiv:0710.3848 (unpublished).
[8] S. Bhattacharjee and K. Sengupta, Phys. Rev. Lett. **97**, 217001 (2006).
[9] J. Linder and A. Sudbø, Phys. Rev. Lett. **99**, 147001 (2007).
[10] A. M. Black-Schaffer and S. Doniach, Phys. Rev. B **75**, 134512 (2007).
[11] B. Kumar and B. S. Shastry, Phys. Rev. B **68**, 104508 (2003).
[12] Q. H. Wang, D. H. Lee, and P. A. Lee, Phys. Rev. B **69**, 092504 (2004).
[13] B. Uchoa and A. H. Castro Neto, Phys. Rev. Lett. **98**, 146801 (2007).
[14] H. B. Heersche, P. Jarillo-Herrero, J. B. Oostinga, L. M. K. Vandersypen, and A. F. Morpurgo, Nature (London) **446**, 56 (2007).
[15] F. Miao, S. Wijeratne, Y. Zhang, U. C. Coskun, W. Bao, and C. N. Lau, Science **317**, 1530 (2007).
[16] X. Du, I. Skachko, and E. Y. Andrei, arXiv:0710.4984 (unpublished).
[17] G. Baskaran, Phys. Rev. B **65**, 212505 (2002).
[18] G. E. Blonder, M. Tinkham, and T. M. Klapwijk, Phys. Rev. B **25**, 4515 (1982).
[19] G. Fagas, G. Tkachov, A. Pfund, and K. Richter, Phys. Rev. B **71**, 224510 (2005).